applied sciences

MDPI

Article

# Experimental Studies and Performance Characteristics Analysis of a Variable-Volume Heat Pump in a Ventilation System

**Anton Frik , Juozas Bielskus , Rasa Džiugaitė-Tumėnienė and Violeta Motuzienė ***

Department of Building Energetics, Vilnius Gediminas Technical University, 10230 Vilnius, Lithuania; anton.frik@vilniustech.lt (A.F.); juozas.bielskus@vilniustech.lt (J.B.); rasa.dziugaite-tumeniene@vilniustech.lt (R.D.-T.)

* Correspondence: violeta.motuziene@vilniustech.lt

**Featured Application: The results of the study may be useful in exploring the extended capabilities of controlling the operational cycle of a heat pump.**

**Abstract:** Air-to-air heat pumps are used in today's ventilation systems increasingly often as they provide heating and cooling for buildings. The energy transformation modes of these units are subject to constant change due to the varying outdoor air state, including temperature and humidity. When choosing how to operate and control energy transformers, it is important to be able to adapt effectively to the changing outside air conditions. Nowadays, modern commercial heat pumps offer two levels of control flexibility: a compressor with a variable speed and an electronic expansion valve. This combination of control elements has boosted the seasonal energy efficiency of heat pumps. For a long time, cycle control possibilities have been dominated by electronic controls. The authors of this paper aim to present an additional element to the traditional heat pump controls, which provides a third level of control over the cycle. To achieve the objective, experimental investigations of a heat pump integrated into a ventilation unit have been carried out under real-life conditions. The experiments involved varying the operating modes of the unit by adjusting the compressor speed, the position of the expansion valve, and the volume of the system loop. The study examined the performance characteristics of the heat pump and found that the performance of a variable-volume heat pump is comparable to that of a conventionally operated typical constant-volume heat pump system. In addition, the study found that by adding a third level of volume control to the active heating circuit, in combination with conventional controls, the heat pump's heat output range could be extended by 69.62%. The study determined the variation of the heat pump cycle in the *p-h* diagram with the variation of the loop volume. The benefits and drawbacks of a heat pump with a variable-volume loop are discussed in this study.

**Keywords:** variable volume air-to-air heat pump; ventilation unit; control level; efficiency; heat pump

check for updates

**Citation:** Frik, A.; Bielskus, J.; Džiugaitė-Tumėnienė, R.; Motuzienė, V. Experimental Studies and Performance Characteristics Analysis of a Variable-Volume Heat Pump in a Ventilation System. *Appl. Sci.* **2024**, *14*, 3933. https://doi.org/10.3390/app14093933

Academic Editors: Daniel Sánchez-García and David Bienvenido Huertas

Received: 3 April 2024

Revised: 1 May 2024

Accepted: 2 May 2024

Published: 5 May 2024

**Copyright:** © 2024 by the authors. Licensee MDPI, Basel, Switzerland. This article is an open access article distributed under the terms and conditions of the Creative Commons Attribution (CC BY) license (https://creativecommons.org/licenses/by/4.0/).

## 1. Introduction

While most countries are implementing policies to increase the energy efficiency of buildings, the average energy consumption per person in the building sector has remained practically unchanged since 1990 [1]. Progress has not been rapid enough to compensate for the growth in the floor area (3% per year) and the increasing energy demand in buildings. Building heating, ventilation and air conditioning (HVAC) systems account for half of the energy consumed in the European Union (EU), much of which is wasted through inefficient use [2].

The heat energy demand of new buildings has significantly decreased with the implementation of heat transfer reduction measures under the Energy Performance of Buildings Directive [3]. At this point, ventilation and air conditioning become the dominant energy use systems in buildings. Additionally, the number of offices is growing both in Lithuania and around the world, leading to a rise in energy consumption. About a quarter of energy use in the buildings sector is accounted for by office buildings, where more than 70% of final energy is consumed by HVAC systems [4]. HVAC systems achieve greater energy efficiency with new monitoring and control technologies [5]. Therefore, these systems specifically require new innovative technological solutions to maintain proper indoor air quality and to use energy efficiently.

New knowledge is needed to identify opportunities for creating more advanced measures that contribute to the EU and Lithuanian strategic goals of reducing energy demand and global greenhouse gas (GHG) emissions through the integration of renewable energy technologies. The primary energy from renewable sources, such as wind energy and solar energy (photovoltaic solar cells), is typically converted into electricity. Since heat pumps require electricity to operate, they become the potential thermal energy generators in HVAC systems, capable of making a contribution to solving the problem of increasing energy efficiency in the building sector. Regarding Zhu et al. [6], the future breakthroughs for integrated renewable energy systems are the use of Machine Learning (ML) with Artificial Intelligence (AI); improved battery technologies to reduce their pollution; a combination of heat pumps and phase change energy storages (PCES); and building design for lower lifecycle emissions. While heat pumps combined with thermal and electrical storages are still under development, further improvements in the efficiency and cost-effectiveness of heat pump technologies are needed. Olympios et al. [7] investigated the performance and cost of different compressor types for small-scale heat pumps (under 30 kW). The authors indicated that rotary vane and scroll compressors resulted in higher coefficient of performance (COP) values (around 3 for rotary vane) at an air temperature of +7 °C, while reciprocating pistons were more competitive at an air temperature of −15 °C (10% higher than scroll). The cost-effective solution for residential buildings is rotary vane compressors for all locations studied. However, for the commercial buildings scroll compressors were the better choice in warm and mild weather, while reciprocating pistons performed slightly better in colder regions. Experimental studies of Wen et al. [8] highlighted the potential of variable-speed control for single screw compressors in heat pumps. By adjusting the motor speed, the authors achieved a balance between efficiency and heating capacity. The study showed that single-screw compressors perform better at relatively high motor speeds. However, the optimal speed depends on the operating conditions, particularly the evaporation temperature. Therefore, for low evaporation temperatures (colder conditions), a combination of higher speed and liquid refrigerant injection can improve the overall performance of heat pump with a single-screw compressor. Wu et al. [9] analysed the optimal selection and design of air source heat pumps (ASHP) based on new parameters, such as the average unit load rate and the comprehensive nominal heating capacity during the heating season. The study showed that a careful selection of ASHP capacities based on building load and using a system with multiple units can significantly improve the overall COP (up to 6%) and energy efficiency of central heating systems. Other research by Koopman et al. [10] provides a detailed air-to-water heat pump simulation model by incorporating an evaporator and condenser pressure drop. The study highlights the influence of ambient conditions, relative humidity, condenser capacity, and refrigerant choice on the COP and pressure drop characteristics for the optimal efficiency of the heat pump. The authors found that the ambient temperature strongly influences the COP: at higher temperatures (20 °C vs. 7 °C), the COP increases by up to 35%; at lower temperatures (−10 °C), the COP decreases. Relative humidity can improve the COP if condensation occurs (up to 10.4% gain). A higher condenser capacity reduces the COP, especially at higher temperatures. The type of the refrigerant affects the pressure drop, which has an impact on the reduction of the COP.

The seasonal energy efficiency ratio is one of the criteria to reduce the energy demand in buildings by improving HVAC systems. In this case, their integral energy performance over the entire operating period depends on both high-rated and instantaneous efficiencies and the ability to maintain them across an extensive range of energy requirements [11].

During the heating season, the prevailing factor is the average outdoor air temperature, and its constant fluctuation affects the seasonal coefficient of performance ($COP_{HP\ SEZ}$) of the heat pump. Recent research by Pineda Quijano et al. [12] shows a growing interest in developing new heat pumping technologies, which assures higher seasonal energy performance. The authors found that magnetocaloric heat pumps with MnFePSi material and dynamic control had a high potential for efficient building heating. Considering motor/drive system efficiency, an estimated system $COP_{HP\ SEZ}$ of 4.5 is achievable.

The integration of heat pump technologies into ventilation systems is a less widespread solution. In recent years, the situation has been changing, with more manufacturers introducing air handling units with integrated heat pumps [13]. However, the operating range of heat pumps integrated into ventilation units is often limited by the outdoor air parameters. And the operating mode ensuring the required supply air temperature is not always efficient and optimal. The control measures of heat pumps have remained unchanged for many years, with the control performed by adjusting the compressor speed and the position of the expansion valve. It is necessary to increase the number of control components to improve the energy efficiency of integrated heat pumps.

### *1.1. Control Methods of Heat Pumps Integrated into Ventilation Systems*

One distinctive feature of HVAC systems is their technologically defined yet constantly stochastic energy demand throughout the year, the day, and sometimes even within hours. The operation modes of heat pumps need to be adjusted depending on the continuously changing ambient temperature. Additionally, decisions must be made regarding the outdoor air temperature at which the highest nominal indicators can be achieved while maintaining system functionality at other temperatures.

Based on the thermodynamic dependencies of fluids, under steady-state conditions, all of the system's state points within the cycle of the heat pump can be defined on the basis of three values of enthalpy at the outlets of the evaporator, compressor, and condenser, along with one pressure or temperature value (corresponding to one of those three enthalpies). To calculate heat transfer quantities, the refrigerant mass flow rate is required. This degree of freedom is a hydrodynamic rather than a thermodynamic variable and cannot be captured in the *p-h* diagram of the cycle. Therefore, the heat pump cycle has a total of four thermodynamic degrees of freedom. Jain and Alleyne [14] presented a case of optimizing these degrees of freedom to reduce the amount of destroyed exergy. It has been theoretically proven that optimization could increase the COP of the refrigeration system by 52.5%. However, optimal operational points of the cycle can be achieved by simultaneously adjusting the system's high and low pressures.

Jensen and Skogestad [15] examined the possible degrees of freedom in the vapor compression cycle from the component perspective. They defined five controllable degrees of freedom: compression work, expansion valve permeability, optimal heat transfer in two heat exchangers, and the "active charge" in the cycle. "Active charge" refers to the mass accumulated in the process equipment, mostly in two heat exchangers. Jensen and Skogestad [15] suggested controlling the amount of "active charge," which indirectly determines the "pressure level" in the cycle. However, others, when optimizing and controlling vapor compression cycle systems, essentially ignored this degree of freedom. Additionally, in this work [15], three out of the five identified degrees of freedom are constrained for technical reasons, leaving the problem of 2 degrees of freedom, where the size of condensation sub-cooling and evaporation superheating is optimized.

In practice, most control methods present the refrigerant mass flow rate and the pressure or temperature of the evaporator to the control system operation. The enthalpies of the condenser and evaporator outlets depend on heat transfer indicators and environmental conditions. The refrigerant flow rate can be controlled by a variable-speed compressor. The state of the evaporator is controlled by a variable-opening expansion valve. This provides two control degrees of freedom. The position of the expansion valve that ensures the required evaporator conditions must depend on a specific operating mode of the refrigerant flow rate (or compressor speed). Most control methods studied by researchers aim to simulate one or both of the abovementioned degrees of freedom, while more advanced controllers focus on manipulating these variables through optimization of the objective function, such as reducing exergy destruction, maximizing the COP, or maintaining heating or cooling loads.

### 1.2. Control Measures

Traditional controls for heat pump operation involve a combination of a compressor and an expansion valve. The compressor operation/capacity can be controlled in several modes: on/off, cascading compressors with different capacities and modulating operation (variable-speed compressor). In modern heat pumps, the combination of a variable speed compressor and a variable position expansion valve is becoming increasingly common. This solution has at times enabled an increase in the seasonal $COP_{HP\ SEZ}$. Continuous advancements are pursued to enhance the $COP_{HP\ SEZ}$.

Modulating (continuous) control is the most appropriate control mode for the compressor in an integrated heat pump system. As there is no thermal accumulation in such systems, the heat pump used for air conditioning must respond immediately to the constantly changing heat demand. Therefore, on/off or stepwise control heat pumps are not suitable for integration into air conditioning equipment. Moreover, as shown by the works of other researchers [16,17], variable-speed operation is more efficient compared to stepwise and on/off operations. Aprea et al. [16] carried out a study of an air-to-water heat pump operating in on/off and modulating modes. The results showed a 20% reduction in electricity consumption for the heat pump using continuous control. Reducing the compression ratio (degrees) during the modulation phase was the main source of energy efficiency [16]. The degradation of efficiency during the on/off cycle operation, under partial load conditions of the heat pump, occurs due to the start-up losses, which depend on the device's characteristics and operating time [18]. Dongellini et al. [17] showed that the seasonal energy efficiency of a heat pump operating in a continuous control mode was 8.3% and 15.4% higher compared to pumps operating in step and on/off modes. In addition, modulating control minimises the number of compressor on/off cycles. This has a positive effect on the compressor's life.

### 1.3. Control Algorithms

Control algorithms for the heat pump cycle can be categorized into conventional, advanced, and smart. Conventional control algorithms are the most widely used type of control algorithm for heat pumps. They rely on fixed set points and simple on/off control logic, making them easy to implement and maintain. However, they may be less efficient and unable to adapt to changing conditions.

Advanced control algorithms are more complex but offer a wider range of features and functionalities. They can consider more variables, such as outdoor and indoor temperature and system operating conditions. They can also use more sophisticated control techniques, such as fuzzy model predictive control (MPC). Advanced control algorithms can improve the efficiency and performance of heat pumps, but they may be more expensive and complex to implement. Chae et al. [19] compared the performance of on/off control and proportional-integral (PI) control for air-to-air heat pumps. The results show that PI control can improve the system's efficiency and stability compared to on/off control. Wang et al. [20] implemented MPC on an air-to-air heat pump and demonstrated its ability to optimize energy consumption while maintaining comfort levels. Hlanze et al. [21] presented a model-based predictive control strategy to optimise the performance of phase change material (PCM) ceiling panels coupled to a multi-stage air-to-air heat pump. Putrayudha et al. [22] applied fuzzy logic control to a ground source heat pump system and showed its effectiveness in improving system performance and user comfort. Yang and Ge [23] presented the effectiveness of a PLC control system and optimized operation strategies in improving a desiccant-coated heat exchanger-based heat pump fresh air system's efficiency

(COP) and dehumidification rate. The study primarily used PID control methods. A PLC control system was developed to manage the system's components. Optimized operation strategies were established for the electronic expansion valve, compressor frequency and switchover period. The results showed an increase in COP of 25% in summer and 78% in winter compared to a non-optimised system.

Artificial intelligence (AI) control algorithms are the most advanced type of control algorithm for heat pumps. They can learn from data and adapt to changing conditions in real-time. They can also integrate with other smart home devices and systems to optimize energy use and comfort. AI control algorithms have the potential to significantly improve the efficiency, performance, and convenience of heat pumps; however, they are still in their early stages of development. Rohrer et al. [24] investigated using deep reinforcement learning (Deep RL) for optimal control of air-source heat pumps, highlighting its potential for significant energy savings.

### *1.4. Experiments on the Improvement of the Vapor Compression Cycle*

The vapor compression cycle has thermodynamic losses in comparison to the ideal reverse Carnot cycle. The compression of a single-phase gas and isenthalpic expansion are related to these losses [25]. The first set of losses results in high refrigerant temperatures, high compression work, and significant heat release in the condenser. When considering the vapour compression cycle for refrigeration purposes, these losses are seen as a negative factor. However, when the cycle is used for heating, some of these drawbacks can be turned into advantages, converting energy losses into useful energy. Additionally, in cold climate zones where air-source heat pumps operate, a high compression ratio is necessary, as it determines the outdoor temperature at which the system can function. The second set of losses leads to significant throttling losses and low refrigeration capacity.

In examining the advancements in vapour compression cycle technologies aimed at reducing thermodynamic losses and improving efficiency/effectiveness, three directions of cycle improvement are distinguished: sub-cooling cycles, expansion loss recovery cycles, and multi-stage cycles.

Research into sub-cooling cycles focuses on the internal heat exchanger of the suction line [26,27], the thermoelectric cooler [28,29], and the mechanical secondary cooler [30,31]. Expansion loss recovery cycles mainly concentrate on expanders (essentially, turbine use) [32,33] and ejectors [34,35] used in vapour compression cycles. Multi-stage cycle studies include vapour or liquid-phase refrigerant injection cycles [36], two-phase refrigerant injection cycles [37], and saturation cycles [38].

Furthermore, the heat pump cycle is examined from the perspective of the discharge temperature of the refrigerant. In one study [39], three cycle improvements were modelled to reduce the compressor discharge temperature. The impact of two-phase refrigerant pumping, liquid-phase injection, and two-phase injection on the compressor discharge temperature was analyzed at fixed condensation and evaporation temperatures. The research shows that all three methods have the potential to reduce the discharge temperature and thus increase the adiabatic efficiency of the compression process. However, two-phase injection outperforms liquid injection and two-phase suction for both heating and cooling efficiency by 4.8% and 11.8%, respectively.

Some researchers aim to improve the efficiency of the vapor compression cycle not through individual cycle measures (directly in contact with the refrigerant) but by altering the parameters of the secondary fluid. In their work [40], the authors presented a heat pump operating in a refrigeration mode with air, pre-cooled by an indirect water vapour cooling condenser, passing through it. Thermodynamically, this solution reduces the refrigerant gas condensation temperature, consequently decreasing the work performed by the compressor. In hot and dry climates, this method can reduce cooling energy consumption by about 20%, but it requires a significant amount of water for the water vapour cooling condenser to function.

Efficiency is sought through a combination of maximizing load selection with modulation and on/off control systems [41], where the use of storage tanks reduces the number of compressor on/off cycles.

An extractable air heat pump or extractable air heat recovery system is essentially an air-to-air heat pump. In cold climate zones, such traditional systems face many problems as the outdoor air temperature drops, including a high-pressure ratio, degradation of the mechanical lubrication properties in the compressor, a decrease in the refrigerant mass flow rate, and a decrease in the heating capacity [42,43].

The mass flow rate of the working fluid in the heat pump is a crucial aspect of the ventilation heat recovery system, affecting its efficiency. As the ratio of condensation and evaporation pressures increases during heat pump operation, the mass flow rate of the refrigerant decreases [44]. This problem is addressed in several ways. One option involves refrigerant vapour injection cycles. Experimental studies [44] show that using such a cycle helps maintain a nearly constant flow rate of the refrigerant passing through the condenser as the outdoor air temperature decreases.

Another option is to use multiple lower-capacity heat pump combinations. In this case, air passes through individual heat exchangers one after another, gradually changing its parameters. This allows for the reduction of the pressure ratio of each heat pump in-volved in the process. This method prevents excessive reduction of the mass flow rate of the working fluid. Additionally, this approach enables exercising control over the heating capacity. Moreover, the problem of a high-pressure ratio can be alleviated by using an ex-tractable air heat pump, as the air passing through the integrated heat pump evaporator in the ventilation system has a higher (indoor) temperature compared to the (outdoor) temperature of the air passing through the condenser. From the perspective of the vapour compression cycle, this means that the refrigerant's evaporation temperature can be higher, and the condensation temperature can be lower compared to a traditional heat pump, where the evaporator is located outdoors, and the condenser indoors. The isotherms of the vapour compression cycle approach each other, eliminating the high compression degree in the cycle, thereby reducing the work performed by the compressor.

Several studies are made to increase the performance of the heat pump compressor with programming. Lee et al. [45] showed a variable-speed control optimization model of the heat pump. Machine learning (ML) was used to predict the thermal load and outdoor temperature, and mixed-integer programming for compressor control optimization. This approach allowed proposing optimal schedules for a heat pump operation in a selected location, reducing its electricity consumption by 9% [45].

Clauß and Georges [46] studied the effect of the complexity and flexibility of the predictive control model of the heat pump on the energy demand of the building. Genetic algorithms (GA) are used to optimise the $COP_{HP\,SEZ}$ by combining the maximum heat pump load, compressor displacement and system operating parameters [47]. However, even in these recent studies, the focus is not on problem-solving by evaluating the possibilities of thermodynamic cycle control, which is the subject of a different set of studies [48]; however, these are specific and not directly related to the characteristics of HVAC systems.

As can be seen from this literature review, the majority of work on improving heat pump efficiency has focused on traditional, well-known and widely used heat pump control measures and their optimal operation strategies. A little attention is given to exploring the thermodynamic cycle of the heat pump and seeking new technological measures to modify and control it. This potential direction could improve the performance indicators of the heat pump integrated into ventilation systems.

The main benefit and novelty of this study is the experimentally proven potential of variable loop volume control technology to improve the performance of a variable-volume heat pump integrated into a ventilation system. The main findings of this study indicate that the control based on volume variation is the most sensitive to the heat output parameters of the heat pump compared to the control based on the compressor or expansion valve.

The variable-volume control technology under investigation may have the potential to extend the operating ranges of integrated heat pumps in the future, which would lead to energy savings in buildings. The goal of the article is to reveal and explore the thermodynamic possibilities of optimally controlling the heat pump cycle integrated into a variable heat demand ventilation system. The research object is the air-to-air heat pump integrated into an air handling unit.

## 2. Materials and Methods

The methodology section discusses the research object and tools.

### 2.1. Subject of the Study

This paper deals with an experimental investigation of an air handling unit (AHU) with an integrated air-to-air heat pump (HP). The theoretical background is also discussed. The schematic diagram of the air-to-air heat pump integrated into a ventilation system is shown in Figure 1. The main components of the experimental bench can be divided into two parts: AHU and HP. The AHU part consists of air ducts with the heat exchangers (condenser and evaporator) and fans of fresh air supply ($F_s$) and air exhaust ($F_e$). The HP part consists of the typical main components as the compressor (CM), the evaporator (EV), the condenser (CN) and the expansion valve (EEV).

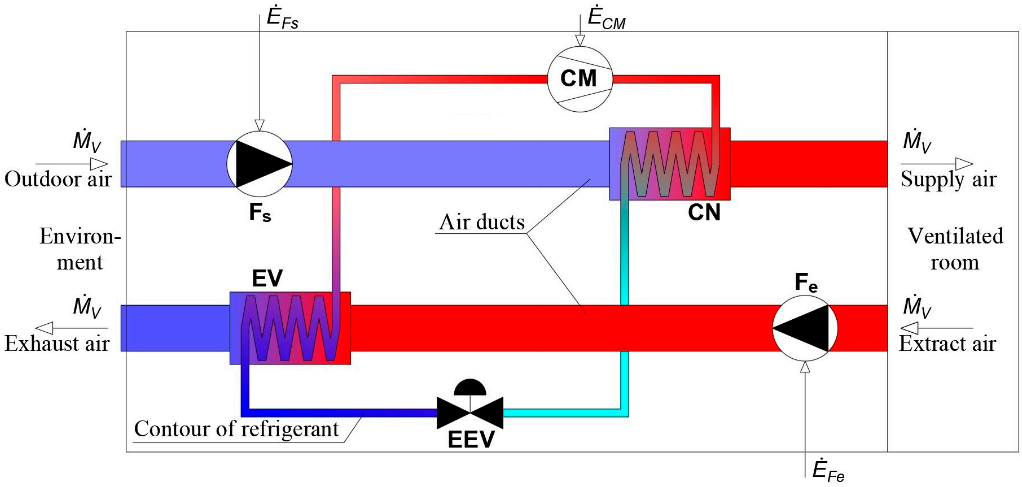


**Figure 1.** The schematic diagram of a ventilation unit with an integrated heat pump.

The theoretical studies were carried out to determine how the evaporation and condensation temperatures vary with the heat pump's heating power (Figure 2). To that end, thermodynamic and parametric analysis were used. The results show the dependencies of the heat pump parameters and their control guidelines.

Figure 2 shows that as the heating power of the HP increases, so does the condensation temperature ($T_{izo\ CN}$), while the evaporation temperature ($T_{izo\ EV}$) decreases, i.e., the isotherms move away from each other as the heating power increases. The increasing temperature difference between the isotherms reflects the increasing pressure difference between the refrigerant in the evaporator and the condenser. The compressor must develop a higher compression ratio. The horizontal dashed line ($T_R$) shows the air temperature supplied to the room as the heat output varies. In this case, the supply air temperature is constant.

In order to obtain the maximum efficiency of the heat pump, it is necessary to vary its parameters as shown in Figure 2. Therefore, in order to determine the possibilities of controlling the heat pump in this mode, an experimental test bench was installed with an additional extension of the control possibilities, i.e., volume variation.

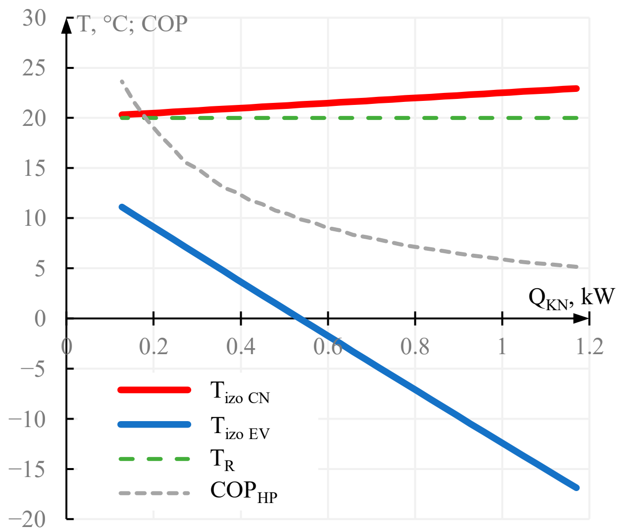


**Figure 2.** The dependence of condensation, evaporation temperatures and the COP on the heating power of HP [49].

### 2.2. Experimental Part

During the study, an experimental set-up was built where, in addition to standard means (compressor speed control, expansion valve position change), the power, condenser and evaporator parameters are also controlled with an introduction of volume change. The schematic diagram of the experimental set-up is shown in Figure 3.

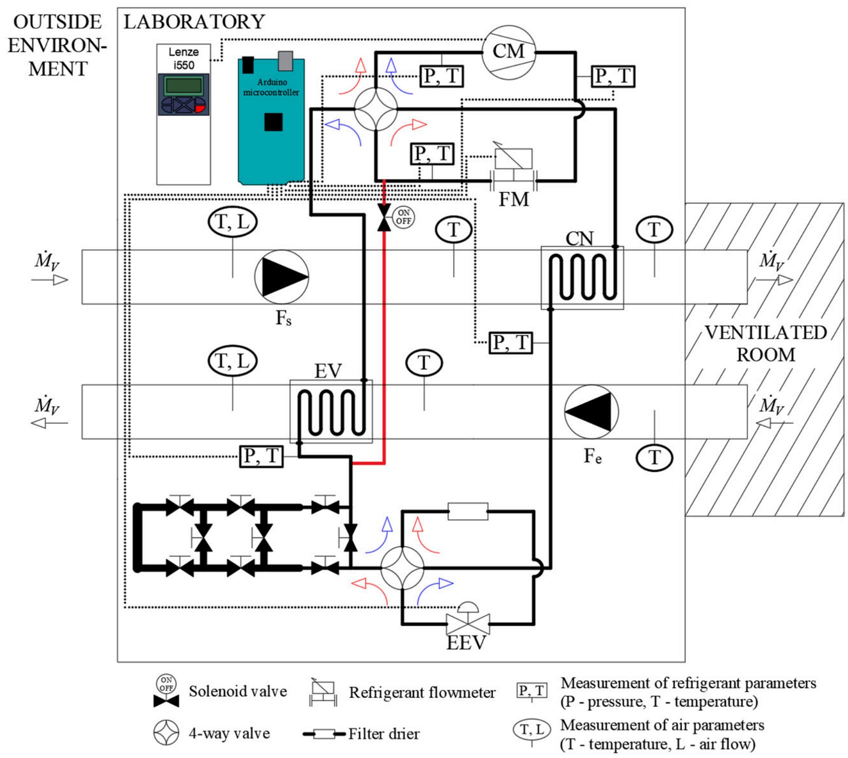


**Figure 3.** The schematic diagram of the experimental test bench with its main components.

Figure 3 shows that the main objective of the operation of the AHU is to provide the required indoor air quality. The purpose of an integrated HP is to recover heat and to preheat the outside air. Table 1 shows the technical characteristics of the main components of the experimental test bench.

**Table 1.** The technical characteristics of the main components of the experimental test bench.

| The Component of the Experimental Bench | Marking in the Diagram | Technical Characteristics |
| --- | --- | --- |
| Supply and exhaust fan RS-315L EC | $F_s$ and $F_e$ | Air flow rate: 430 $m^3/h$ |
| EC-10 Fan motors potentiometer | - | Control signal: 0–10 V |
| Heat pump compressor GMCC (Foshan, China) YA281X3CS-4MT | CM | Refrigerant: R410A; voltage: 380–415 V; heating capacity: 6.92 kW |
| Frequency inverter Lenze i550 | - | Voltage: 380–415 V |
| Expansion valve Carel (Breganze, Italy) E2V14 BSF01 | EVV | Maximum differential pressure: 35 bars; full closing steps: 480. |
| Condenser | CN | DX coil heat exchange surface: 4.5 $m^2$; air flow rate: 400 $m^3/h$, pressure drop: 25 Pa |
| Evaporator | EV | DX coil heat exchange surface: 5.9 $m^2$; air flow rate: 400 $m^3/h$, pressure drop: 18 Pa |
| Microcontroller board Arduino Mega 2560 | - | Operating voltage: 5 V; digital I/O: 54; analog input: 16; flash: 256 KB; SRAM: 8 KB. |

The test bench is equipped with two four-way valves to allow the HP to be used for cooling. A hot steam line is installed to defrost the evaporator when it freezes. This paper presents a study addressing only the heating season. The speed of the compressor is changed using a Lenze (Hamelin, Germany) i550 frequency converter. The expansion valve position is changed using an Arduino (Ivrea, Italy) Mega 2560 microcontroller board.

This experimental bench has the advantage of being equipped with a multi-stage volumetric enlarger, which allows the system volume to be increased. The multi-stage volumetric enlarger is located between the evaporator (EV) and the electronic expansion valve (EEV). A schematic diagram of the multi-stage volumetric enlarger is shown in Figure 4.

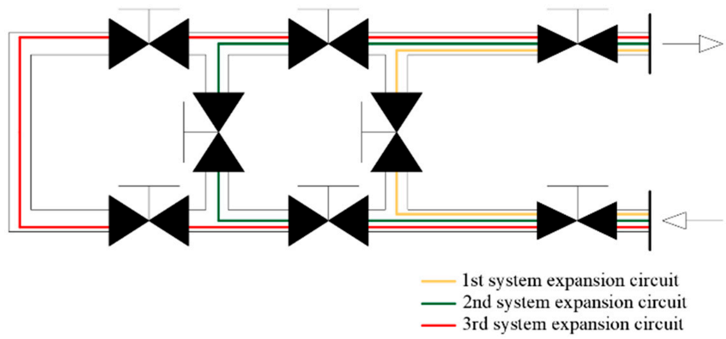


**Figure 4.** A multi-stage volumetric enlarger for increasing the volume of a heat pump.

The multi-stage volumetric enlarger consists of a number of shut-off ball valves and piping. The combination of these components allows the internal volume of the heat pump to be gradually increased by 17.0% (+0.81 $dm^3$) (V1), 26.4% (+1.26 $dm^3$) (V2), 34.4% (+1.64 $dm^3$) (V3) in relation to the initial volume (V0 = 4.76 $dm^3$). A test cycle is performed with the volume expansion. After the cycle, the volume is increased and the test is repeated.

Figure 5 presents the images of the experimental test bench.

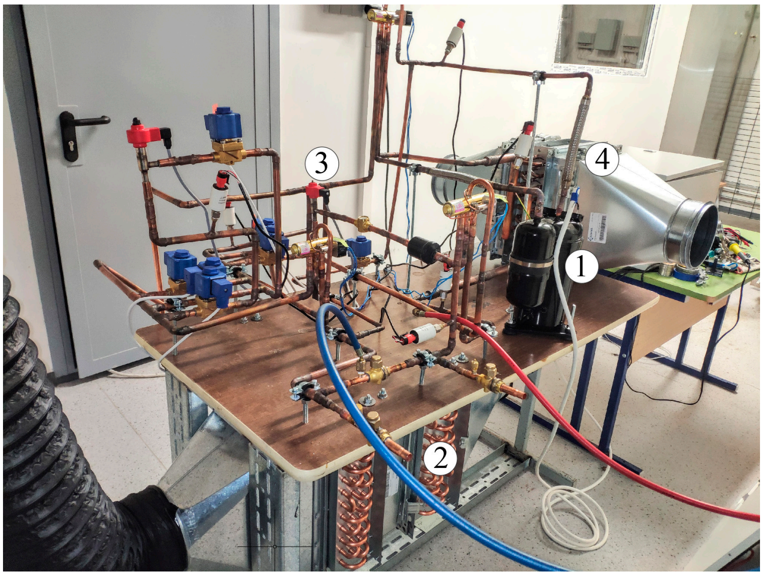


(a)

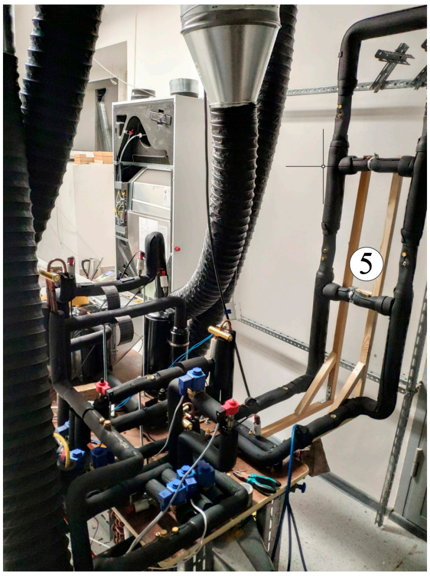


(b)

**Figure 5.** Digital photos of the experimental bench: (**a**) the experimental bench without thermal isolation and volume expansion; (**b**) the experimental bench with thermal isolation and a volume expansion unit.

Figure 5 shows digital photos of the experimental test bench where part (a) shows the experimental bench at the production stage, when there is no thermal insulation or volume expansion installed yet, and part (b) shows the bench, which is insulated and equipped with volume expansion and additional components, such as flexible ducts that supply and extract air. In addition, the main components are presented and marked in the pictures: (1) the compressor; (2) the evaporator; (3) the expansion valve; (4) the condenser; and (5) the volume expansion unit.

The following section discusses the measurement tool used to record the performance of the device.

### *2.3. Measuring Equipment*

This study used a large number and variety of measuring equipment. During the study, a large number of values were recorded and an energy balance was constructed to determine whether the measurements were accurate. Below is a list of the measurement equipment used (Table 2).

**Table 2.** Used measurement equipment.

| Name of Measuring Equipment | Properties | Notes |
|---|---|---|
| AHLBORN (Goettingen, Germany) ALMEMO 2890-9 measuring instrument and data logger | Measuring inputs: 9; Outputs: 2; Memory: 100,000 measured values | Used to record differential air pressure values. |
| Pressure measuring connector for differential pressure FDA 602 S1K | Measuring range: ±1250 Pa; Operating range: −10 to +60 °C, 10 to 90% RH; Accuracy: ±0.5% of the final value in the range of 0 to the final positive value | Measures the pressure difference across the airflow measurement diaphragm. |
| 160 mm diameter airflow calibrated diaphragm | Measuring range: nominal air flow 400 $m^3/h$; Difference pressure: 400 Pa at nominal air flow; Accuracy: ±0.66% at 400 $m^3/h$ | The length of the straight section upstream of the measurement point is 12 diameters; downstream, 6 diameters. |

**Table 2.** *Cont.*

| Name of Measuring Equipment | Properties | Notes |
|---|---|---|
| Multi-channel data logger Onset (Burlington, MA, USA) Hobo H22-001 | Measuring inputs: 3 FlexSmart multi-channel modules and up to 6 Smart Sensors;<br>Outputs: 2;<br>Operating range: −40 to +60 °C;<br>Memory: 512K nonvolatile flash data storage. | Used to record temperatures and electricity parameters |
| 12-Bit temperature smart sensor | Measuring range: −40 to 100 °C;<br>Accuracy: ±0.2 °C from 0° to 50 °C. | Measures air and freon temperature. Connects to Hobo H22-001 |
| 3-Phase AC kWh transducer sensor onset T-VER-8044-100 | Measuring range: 0 to 100 A;<br>Operating range: 0 to +60 °C, 0 to 95% RH;<br>Input primary voltage: 480 Volts AC rms;<br>Output: 4–20 mA;<br>Accuracy: ±1% per ANSI (from 10 to 100% of CT rating). | Connects to Hobo H22-001 |
| Pressure sensors Sanhua (Shaoxing, China) YCQC05L09 | Measuring range: 0 bar to 44.8 bar;<br>Operating range: −40 to +80 °C, max. working pressure 75 bar;<br>Output: 4–20 mA;<br>Accuracy: ±0.8% FS. | Used with Arduino Mega 2560 |

The following parameters were recorded during the experimental studies:

- refrigerant pressures, temperatures and flow rates;
- airflow (determined by using the calibrated diaphragms), temperature and relative humidity.

The tests were carried out under realistic climatic conditions and measurements were taken at 10 s intervals. Figure 3 shows the locations of the installed sensors and the recorded parameters.

An experiment is conducted to determine how the operating parameters of the heat pump change when it is controlled by three control measures: compressor, expansion valve, and circuit volume. Throughout the study, the heat pump operates under different combinations of these three control components: the compressor speed is varied between 1800, 1920, 2100, and 2220 rpm; the expansion valve permeability is varied between 30%, 50%, and 70%; the system volume is varied between V0 and V4. All combinations of control component parameters throughout the experiment are presented in Table 3.

**Table 3.** Combinations of heat pump control component parameters.

| Volume | Speed of Compressor (rpm);<br>Opening Degree of Expansion Valve (%) | | | | | | | | | | | |
|---|---|---|---|---|---|---|---|---|---|---|---|---|
| V0 | 1800; 30 | 1920; 30 | 2100; 30 | 2220; 30 | 1800; 50 | 1920; 50 | 2100; 50 | 2220; 50 | 1800; 70 | 1920; 70 | 2100; 70 | 2220; 70 |
| V1 | 1800; 30 | 1920; 30 | 2100; 30 | 2220; 30 | 1800; 50 | 1920; 50 | 2100; 50 | 2220; 50 | 1800; 70 | 1920; 70 | 2100; 70 | 2220; 70 |
| V2 | 1800; 30 | 1920; 30 | 2100; 30 | 2220; 30 | 1800; 50 | 1920; 50 | 2100; 50 | 2220; 50 | 1800; 70 | 1920; 70 | 2100; 70 | 2220; 70 |
| V3 | 1800; 30 | 1920; 30 | 2100; 30 | 2220; 30 | 1800; 50 | 1920; 50 | 2100; 50 | 2220; 50 | 1800; 70 | 1920; 70 | 2100; 70 | 2220; 70 |

The experiment commences with the smallest system volume, compressor speed, and expansion valve permeability (V0, 1800 rpm, 30%), during which the operating parameters of the heat pump (refrigerant pressures, temperatures) are observed to remain constant for 10 min, indicating a steady-state process. Subsequently, the compressor speed is increased to 1920 rpm, and again, the process is allowed to stabilize. This approach is applied to all combinations of certain expansion valve and compressor speed settings. Once all compressor speeds have been examined, the expansion valve permeability is increased, and the compressor speed is varied again from 1800 rpm to 2220 rpm.

Meanwhile, when all combinations of compressor speed and expansion valve permeability have been explored, the system volume is increased from V0 to V1, and tests are repeated, varying the speed and the permeability. This process yields all operational results for the heat pump (48 data points). Parameters for further analysis of each operating combination are based on the average of the parameters measured during a steady-state period of 10 min.

### 2.4. Determining the Actual Performance Parameters of the HP from a Theoretical Model

The experimental study generates a large amount of data, which is processed and structured in the results section to produce the final result.

In this work, the compressor is a major focus, so its compression ratio is used in the data analysis, which determines its performance and efficiency. The compressor compression ratio is calculated as follows:

$$Compression\ Ratio = \frac{P_1}{P_2}, \tag{1}$$

where $P_1$ is the inlet pressure and $P_2$ is the outlet pressure.

A heat pump has more components than just the compressor. Therefore, the heat pump performance is characterized by other quantities, such as the amount of heat (or power) produced, the amount of electricity consumed and its COP.

The heating capacity provided by the heat pump is evaluated as follows:

$$\dot{Q} = \dot{M} \cdot c_p \cdot (T_{out} - T_{in}) = \dot{M} \cdot (h_{out} - h_{in}), kW \tag{2}$$

where $M$ is the air mass flow rate, kg/s; $c_p$ is the fluid specific heat, kJ/(kg·K); $T_{out}$ and $T_{in}$ are the end and start temperatures of the process, K; and $h_{out}$ and $h_{in}$ are the enthalpies of the process at the end and at the start of the process, kJ/kg.

The above formula is suitable for determining the heat quantities and capacities for different types of working material, i.e., both air and refrigerant.

The overall COP of the heat pump is determined as follows:

$$\text{COP} = \frac{\dot{Q}}{\dot{E}} \tag{3}$$

where $Q$ is the quantity of heat produced by the heat pump (supplied to the room), kW (or kWh); $E$, the amount of electricity withdrawn to produce the amount of heat, in kW (or kWh). The electricity consumed by the installation shall be recorded in kWh according to the power factor.

## 3. Results and Discussion

In this study, a ventilation system with an integrated heat pump was tested. The ventilation unit does not use a heat recovery heat exchanger. The heat recovery function is performed by the heat pump. The main purpose of the heat pump is to extract heat from the exhaust air and to warm the cold air supplied from the outside. All tests are carried out under real-life climatic conditions and the control of the heat pump has been extended with additional functions.

A volume expansion device is implemented in the heat pump circuit, which allows the initial volume of the refrigerant circulating circuit to increase by 17.0% (+0.81 dm$^3$) (V1), 26.4% (+1.26 dm$^3$) (V2), and 34.4% (+1.64 dm$^3$) (V3) in comparison with the initial system volume V0 (4.76 dm$^3$). The tests are carried out at different speeds of the HP compressor and at different expansion valve capacities. The compressor speeds are 1800, 1920, 2100, and 2200 rpm. The expansion valve flow positions are 30%, 50%, and 70%. The heat pump circuit uses 1.13 kg of R410A refrigerant.

### 3.1. General Characteristics

In this subsection, the typical performance of an experimental heat pump is present-ed. The purpose is to determine how the heat pump performs when controlled by standard means in combination with the system volume change and to make a comparison with the characteristics of several compressors provided by the manufacturers.

#### 3.1.1. The Degree of Compression and Flow Rate

One of the typical characteristics of heat pump compressors is the dependence of the degree of compression (the ratio of the refrigerant pressure upstream and downstream of the compressor) on the mass flow rate of the refrigerant. Figure 6 shows the operating points obtained during the experiment and Figure 7 shows the operating points of different compressors as declared by the equipment manufacturers.

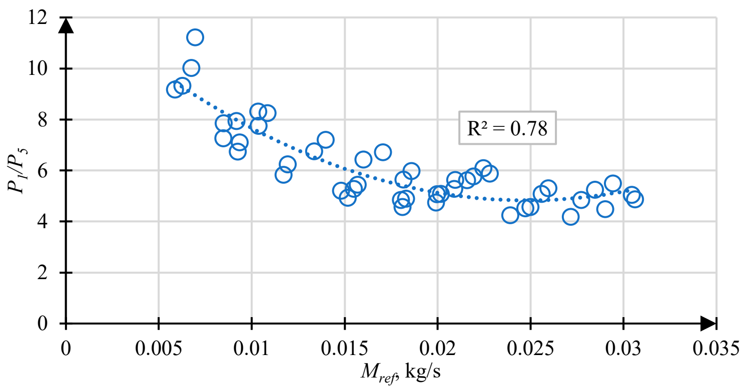


**Figure 6.** The relationship between the compressor pressure ratio $P_1/P_5$ and the flow rate (experimental data).

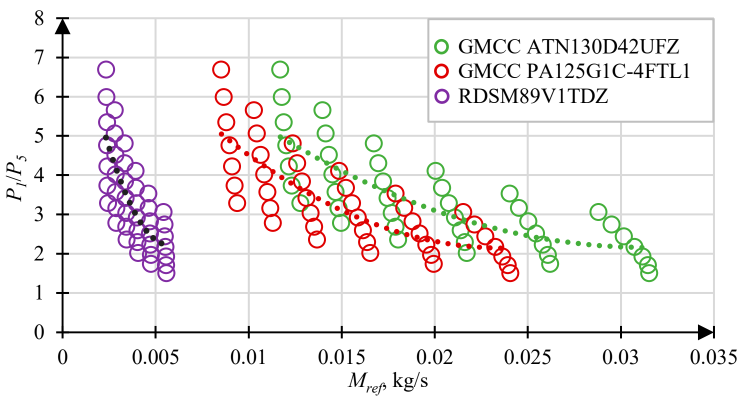


**Figure 7.** The relationship between the compressor pressure ratio and the flow rate (manufacturers' data).

As mentioned above, Figure 6 shows, in circles, the points of dependence of the refrigerant compression ratio on the flow rate for heat pump compressors from different manufacturers, and the dotted line shows the regression equation for these compressor-specific points, which is generated by a second-degree polynomial.

It can be seen that the trend of the compression ratio reported by the compressor manufacturers (Figure 7) is in line with the values obtained during the experiment (Figure 6).

Observably, as the refrigerant flow rate increases, the degree of compression generated decreases. A similar trend was observed during the experiment.

### 3.1.2. Flow Rate and Evaporation Temperature

Another characteristic of heat pumps is the dependence of the refrigerant flow rate on the evaporation temperature. Figure 8 shows this characteristic for an experimental heat pump obtained during testing. It can be seen that a higher evaporation temperature leads to a higher flow rate through the system.

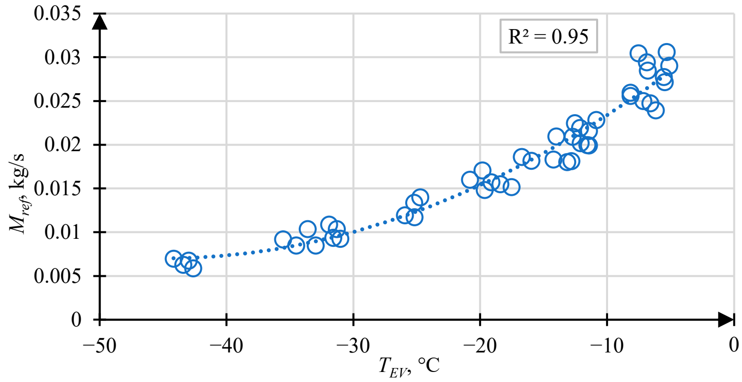


**Figure 8.** The relationship between the refrigerant flow rate and the evaporation temperature (experimental data).

Figure 8 shows that as the evaporation temperature increases, so does the flow rate. These points are joined by a regression line, which is a second-degree polynomial and the resulting regression rate is greater than 95%. This value indicates that the regression equation reproduces the measurement points with sufficient accuracy to allow the equation to be used in place of the measurements in further studies. Figure 9 shows the curves provided by the compressor manufacturers.

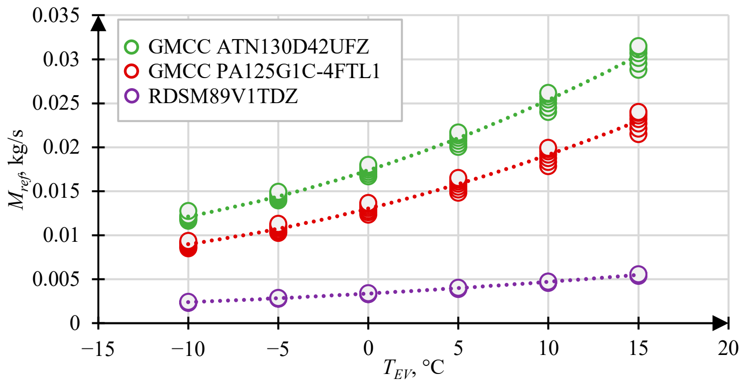


**Figure 9.** The relationship between the refrigerant flow rate and the evaporation temperature (manufacturers' data).

Figure 9 shows a trend similar to the experimental results. This similarity indicates that the results of the experimental studies are sufficiently accurate. The power and flow rate dependencies are then presented in the next subsection.

### 3.1.3. Power and Flow Rate

Another characteristic parameter of a heat pump is the dependence of the heating power on the mass flow rate. Figures 10 and 11 present these characteristics obtained from experimental tests and data from different manufacturers, respectively.

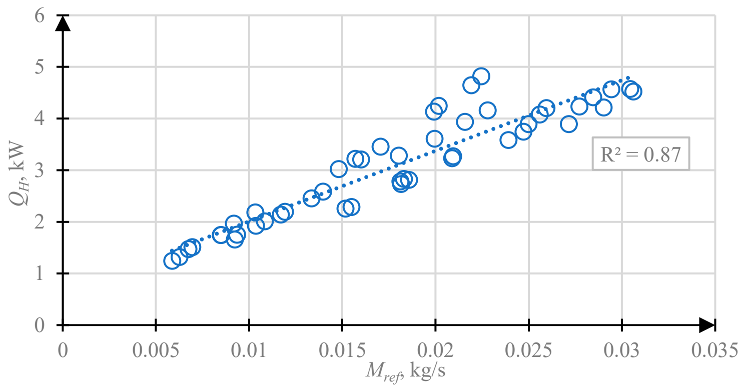


**Figure 10.** Heating power vs. flow rate (experimental data).

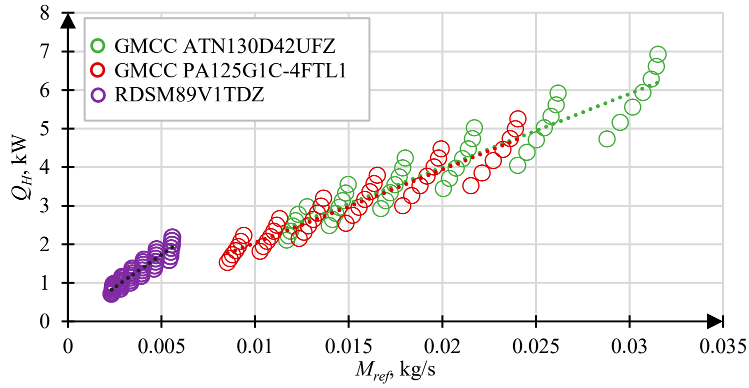


**Figure 11.** Heating power vs. flow rate (manufacturers' data).

Figure 10 shows that as the flow rate increases, so does the power of the heat pump, and when the points are connected by a regression line, a regression coefficient of over 87% is obtained. This coefficient shows that the performance can be calculated with sufficiently high accuracy. The figures below show the performance data from compressor manufacturers.

From Figure 11, it can be seen that the compressor performance characteristics are similar to Figure 10, which again shows that the experimental studies repeated by the authors are logical and can be trusted.

### *3.2. The Effect on the Performance Parameters of a Change in the Heat Pump Circuit Volume (V0, V1, V2, V3)*

This section presents the results of experimental tests where the volume of the system is changed but the mass of the refrigerant is kept constant. The refrigerant pressure is 11 bar when the heat pump system is not operating. The tests start from the smallest system volume. The test results are presented starting with the variation of the heating capacity of the heat pump at different system loop volumes.

#### 3.2.1. Heating Power

One of the most common descriptors of how heat pumps work is the heating capacity. In this case, the figure below shows how the heating power varies at different compressor speeds, throttle positions, and volumes of the HP system. The heating power was evaluated by measuring the air flow rate and the temperatures before and after the condenser.

Figure 12 shows that by adjusting the heat pump operation using conventional methods in the baseline case with a loop volume of V0, a range of supplied air heating capacity from 3.89 kW to 4.82 kW is achieved with a change of 0.93 kW. Increasing the volume of the HP loop by 17.0% (from V0 to V1), the heating power at the lowest speed and low flow rate is 3.02 kW. Increasing the speed and the flow rate of the expansion valve, the heat output gradually increases to 4.21 kW. There has been an increase in power, but fluctuations have also been observed, potentially due to the different speeds and flow rates. It can be seen that the power range (compared to the V0 case) has widened by 27.66% (from 0.93 to 1.18 kW), but the overall limits of the achieved power control range have decreased, compared to the baseline, from 3.02 kW to 4.21 kW. The trend remained unchanged with further increases in system volume. For V2, the loop volume increased by 26.4% to 6.01 dm$^3$, and for V3 by 34.4% to 6.40 dm$^3$ compared to the baseline (case V0). For case V2, the control range of the heating power increased by 65.15% (from 0.93 to 1.53 kW), and for case V3 by 69.62% (from 0.93 to 1.57 kW) compared to the baseline case. On the other hand, the overall limits of the achieved power control range decreased by 1.74 to 3.27 kW and by 1.25 to 2.82 kW for V2 and V3, respectively.

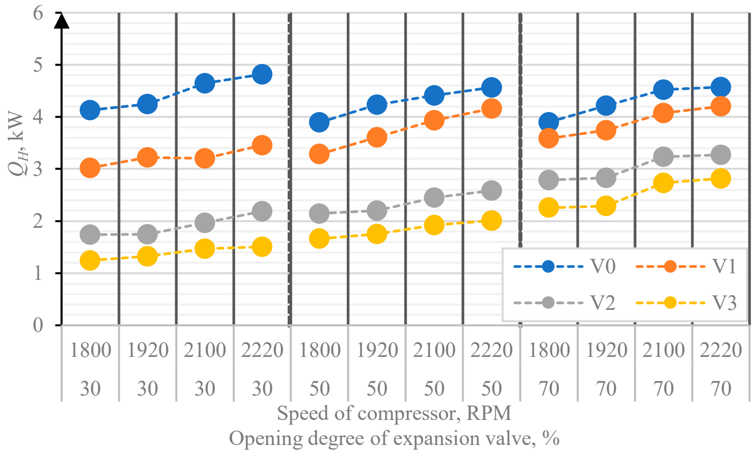


**Figure 12.** The heating power of the HP during the experiment.

It is noted that the use of additional controls by varying the volume of the heating circuit, in combination with conventional control measures, has allowed the heating power range to be extended, i.e., the difference between the maximum and the minimum power is achieved by varying the speed of rotation and the throttle capacity. This increase in the power range is as much as 0.7 times compared to the V0 case. It can be concluded that the volume expansion reduces the maximum heating power of the unit but allows it to be controlled over a wider range. A wider control range may be useful in cold climates during transition periods when a low HP output is required, which means that buffer capacity can be avoided. A buffer capacity is built in when the selected high-capacity HP cannot operate at low capacities, while the expansion of the volume reduces the power and increases the control range. This paper does not analyse the heat pump performance in the long term or in transient periods: this will be investigated in the next steps.

### 3.2.2. Efficiency

Adjusting the volume of the HP loop has allowed extending the range of the available heating power, but the general trend is that the COP decreases with the HP loop volume going up. The average COP for each volume increase dropped by 5.14% (V1), 18.03% (V2) and 26.53% (V3) compared to the base case V0 (Figure 13).

Figure 13 shows that in most cases, increasing the bandwidth and having a low speed slightly increases the efficiency for V0, V2 and V3. For V2 and V3, the highest efficiency is achieved with this style of operation.

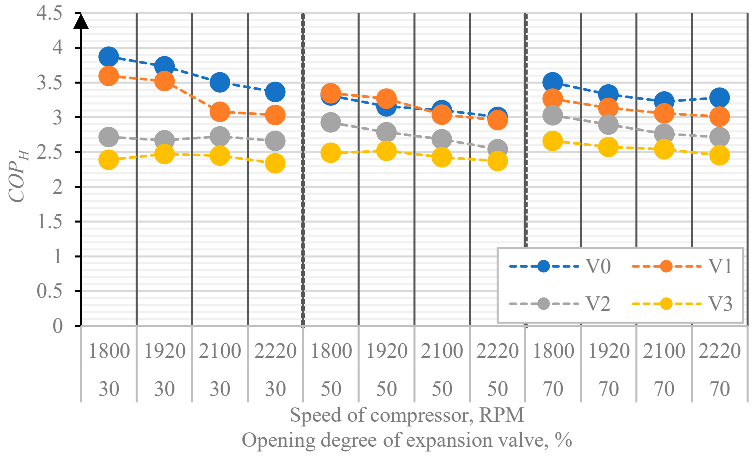


**Figure 13.** The COP during the experiment.

However, it has been observed that the variation in performance is also dependent on the outside air temperature, which shapes the fluctuations. The variation of the outdoor temperature has a negligible effect on the heating power achieved by the heat pump, with a regression coefficient of 0.36 (Figure 14a), but the performance coefficient has been observed to be more sensitive to the outdoor air parameters, with a regression coefficient of 0.49 (Figure 14b).

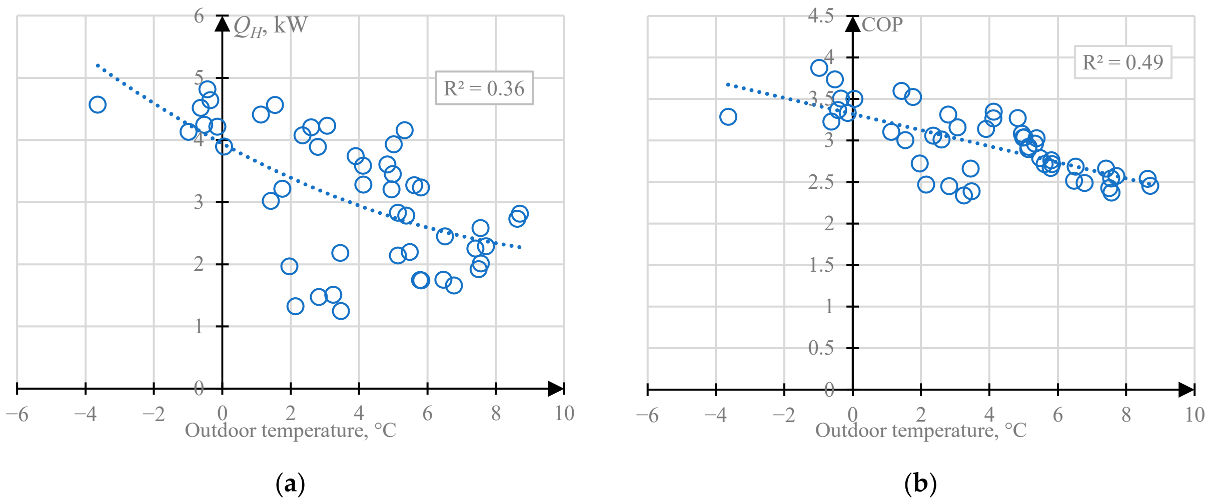


**Figure 14.** The dependence of the heat pump parameters on the outside air temperature: (**a**) heating power vs. outdoor air temperature; (**b**) COP vs. the outdoor air temperature.

Additionally, one general trend has been noted, where the efficiency of the heat pump increases with the outdoor air temperature decreasing. This is not a typical trend for heat pumps, and it may be due to the installed compressor power, which is higher to ensure a higher efficiency even when the outdoor air temperature is very low.

From the above results, it can be seen that increasing the loop volume enables the heat pump to operate at a lower heating capacity than in the initial case (V0). This means that the change of the heat pump circuit volume has resulted in a wider range of heating power. This allows the unit to operate with a decent amount of stability over a wider range of outdoor air temperatures. However, there is a downside to increasing the volume of the heat pump circuit, as it decreases the efficiency of the HP; however, the effect of the third stage on the seasonal efficiency has not been investigated. The evaluation of the seasonal performance factor will be carried out in future work where its performance in a real system with real heat demands will be simulated.

With a strong increase in volume (cases V2 and V3), a phenomenon that has similarities with cases where there is partial leakage of the refrigerant from the heat pump system is observed [50,51]. It is therefore appropriate in future studies to add more refrigerant to the system than recommended and subsequently have a significantly higher performance potential.

### 3.3. Heat Pump Cycles in a p-h Diagram

The previous part of the results showed how increasing the system volume affects the output and the performance of the plant. This subsection shows the characteristic changes in the heat pump operation cycle in a *p-h* diagram when the plant is operated in the above-mentioned fashion. The graphs below are based on the experimental results.

Figure 15 shows a typical case of compressor control, with constant expansion valve capacity at 70%, the compressor speed varying between 1800 and 2220 (intermediate cycles of 1900 and 2100 are not shown), and the heat pump loop volume of V0. It can be seen that the variation of the compressor speed has a small effect on the differences between the superheating and sub-cooling temperatures of the cycle, which remain similar. In addition, increasing the compressor speed increased the condensation temperature and decreased the evaporation temperature. This trend comes into light because increasing the compressor speed results in a higher rate of refrigerant flow through the compressor, which also results in a higher flow rate through the expansion valve, and a lower pressure is generated behind the expansion valve than at speed. It can therefore be argued that the change in the compressor speed has a direct influence on the operating mode of the evaporator. Similar trends can be seen in other throttle cases as well.

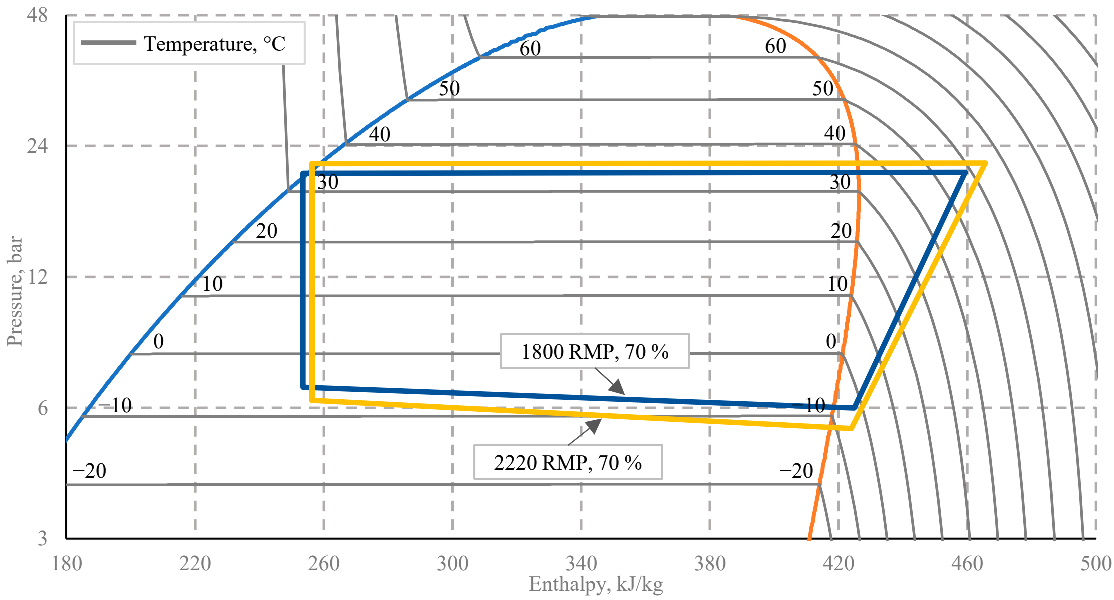


**Figure 15.** The operation cycles of the HP in a *p-h* diagram (compressor speeds: 1800 and 2220 rpm; expansion valve capacity: 70%; volume: V0).

Figure 16 shows a case where the heat pump is controlled by an expansion valve, its flow rate varying between 30% and 70%, with a fixed compressor speed and a fixed volume of the HP loop at V0. The change of the expansion valve flow rate had a negligible effect on the condensing temperature (the difference between the limiting cases is 2.75 °C), but a more significant effect on the evaporating temperature of 6.83 °C between the valve flow rate cases of 30% and 70%. In addition, controlling the heat pump with the expansion valve was able to affect the superheating and sub-cooling temperatures of the cycle. Reducing the valve permeability from 70% to 30% resulted in an increase in the differences between the superheating and sub-cooling temperatures of 19.33 °C and 6.87 °C, respectively. Therefore, the position of the expansion valve has a significantly greater impact on the operating mode of the evaporator than the case of changing the compressor mode.

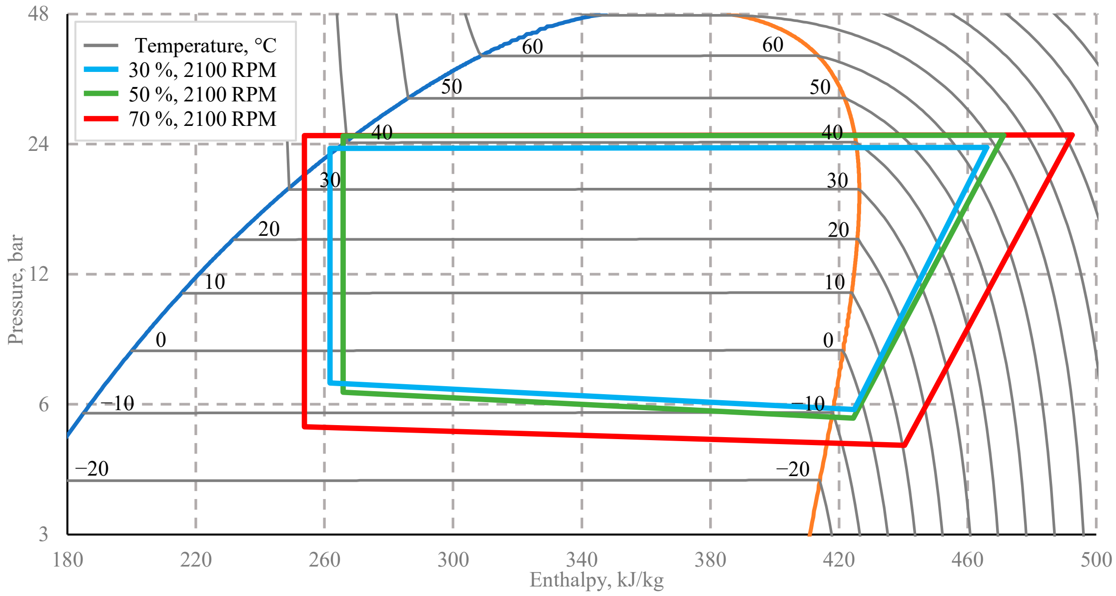


**Figure 16.** The operation cycles of the HP in a *p-h* diagram (compressor speed: 2100 rpm; expansion valve capacity: 30, 50, 70%; volume: V0).

Changing the volume of the heat pump circuit had the most significant effect on the heat pump operation cycle (Figure 17). Increasing the volume from V0 to V1 resulted in a virtually uniform "lowering" of the cycle in the graph. In this case, the condensation and evaporation isotherms were reduced by 8.30 °C and 8.22 °C, respectively, while the temperatures upstream and downstream of the compressor were similar. As the system volume was further increased to V2 and V3, the condenser and evaporator lines moved steadily in the direction of the pressure drop. However, the cycles did not reach/pass into the two-phase region, which means that no refrigerant condensation process occurred in the condenser and the whole cycle was in the superheated vapour region. The high temperature and pressure vapour leaving the compressor was cooled but not condensed in the condenser. In these cases (V2, V3), the enthalpy differences between the condenser and the evaporator were reduced by several times compared to the cases V0 and V1.

From the *p-h* diagrams, it can be seen that changing the volume of the system extends the operating range compared to standard measures. An increase in volume by 17% improves the controllability, but an increase in volume by more than 26% is detrimental to the performance as no evaporation or condensation are achieved. This benefit of volume variation can also be applied to cooling or refrigeration processes, since neither the compressor speed nor the throttle capacity is altered, and increasing the volume lowers the evaporating temperature with almost no change in the performance. An average reduction in the COP from V0 to V1 for a volume increase of 5.14% is observed.

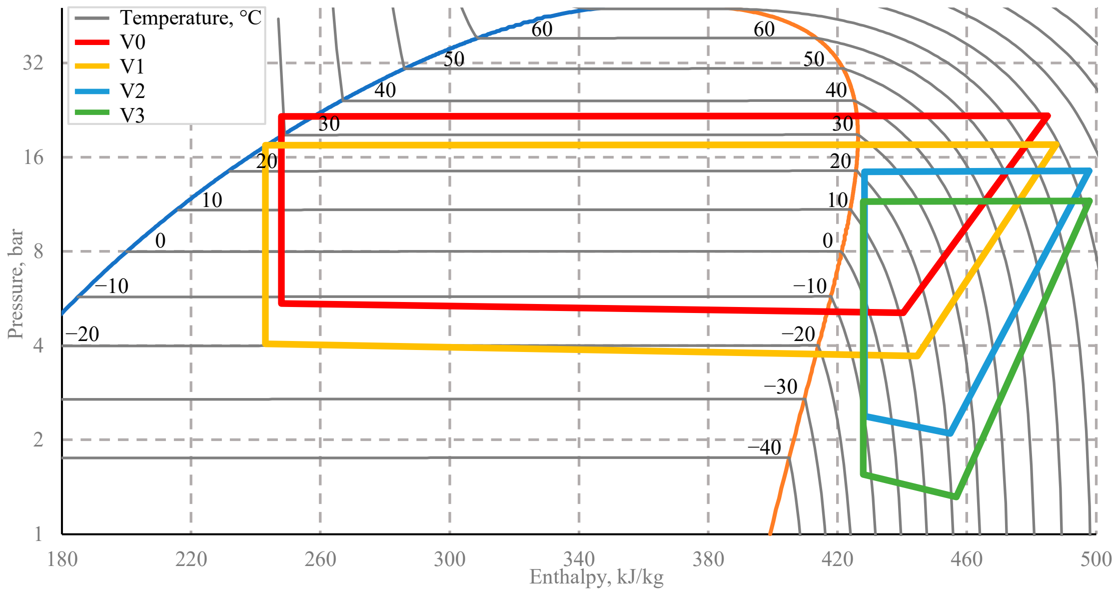


**Figure 17.** The operation cycles of the HP in a *p-h* diagram (compressor speed: 1800 rpm; expansion valve capacity: 30%; volumes: V0, V1, V2, V3).

## 4. Conclusions

This article presents experimental studies of a heat pump integrated into a ventilation unit. The experiments involved varying the operating modes of the unit by changing the compressor speed, the position of the expansion valve, and the system volume. The comparison of the performance characteristics showed that the performance trends of the variable-volume heat pump are similar to those of the typical constant-volume heat pumps controlled by standard means (compressor and expansion valve). The experimental results show that the trends are similar, indicating a sufficient degree of accuracy.

Additional control was achieved by changing the volume of the heat pump circuit, which, when combined with conventional controls, extended the heating power range. Increasing the volume of the system loop enables the heat pump to operate at a lower heating capacity than in the original case (V0), allowing the unit to operate with stability over a wider range of outdoor air temperatures.

Increasing the volume of the heat pump loop was found to decrease its efficiency. This phenomenon is similar to the case of partial refrigerant leakage from the heat pump system.

The analysis of the experimental heat pump operation cycles in a pressure-enthalpy diagram revealed that altering the compressor speed had a negligible impact on the temperature differences between the superheating and sub-cooling stages of the cycle. Increasing the compressor speed raises the condensation temperature and lowers the evaporation temperature. On the other hand, modifying the flow rate of the expansion valve has a more pronounced effect on the evaporation temperature than on the condensation temperature. The superheating and sub-cooling temperatures of the cycle were influenced by adjusting the heat pump with the expansion valve. An increase in the difference between these temperatures was achieved by reducing the valve's permeability. The operation cycle of the heat pump was significantly affected by increasing the volume of the heat pump circuit. Increasing the volume can lead to a more uniform "lowering" of the cycle in the diagram, resulting in lower temperatures for the condensation and evaporation isotherms.

However, it is important to note that controllability is positively affected when the increase in volume is 17% or less. Beyond this point, performance is negatively impacted as the evaporation and condensation process cannot be achieved. Volume variation can benefit the cooling or refrigeration processes without altering the compressor speed or throttle capacity. By increasing volume, the evaporating temperature can be lowered with minimal impact on the operating efficiency.

Experimental investigations have revealed a significant influence of control components on the performance of a variable-volume heat pump. When controlled by varying the volume, the heating capacity parameters of the heat pump respond with the highest degree of sensitivity compared to control by the compressor or expansion valve. This sensitivity indicates the potential for developing novel control methods and components through the implementation of variable circuit volume technology in heat pump regulation. Since there are few new heat pump control components emerging in commercial devices (with only the existing components being improved instead), this technology could expand the operating ranges of heat pumps in the future, thereby helping to reduce energy consumption during their production and operation.

This study represents initial steps in exploring the potential of variable-volume heat pump control. Future research is recommended to investigate the volume change control of the heat pump over a wider range of outdoor air temperatures, as well as in devices of different capacities. Additionally, it is worth analysing the adaptability of this volume change method in refrigeration equipment, since it has been established that an increase in volume, with constant compressor speed and expansion valve position, reduces the evaporation temperature with almost no change in performance.

During the subsequent stages of the study, analysis will be conducted on the long-term operation of a heat pump with a variable circuit volume in the ventilation system, considering its performance during transition periods and assessing seasonal efficiency indicators.

**Author Contributions:** Conceptualization, A.F., J.B., R.D.-T. and V.M.; methodology, A.F. and J.B.; software, A.F.; validation, A.F. and J.B.; formal analysis, A.F.; investigation, A.F.; data curation, A.F.; writing—original draft preparation, A.F., J.B. and R.D.-T.; writing—review and editing, A.F., J.B., R.D.-T. and V.M.; visualization, A.F. and J.B. All authors have read and agreed to the published version of the manuscript.

**Funding:** This research received no external funding.

**Institutional Review Board Statement:** Not applicable.

**Informed Consent Statement:** Not applicable.

**Data Availability Statement:** The data presented in this study are available on request from the corresponding author.

**Acknowledgments:** The authors are thankful to Vytautas Martinaitis for the inspiration, useful discussion of theoretical frameworks, and valuable and constructive suggestions during the planning and development of this study.

**Conflicts of Interest:** The authors declare no conflicts of interest.

## References

1. International Energy Agency. *Market Report Series: Energy Efficiency 2O17*; IEA Publications: Paris, France, 2017; pp. 1–143. Available online: https://www.iea.org/reports/energy-efficiency-2017 (accessed on 1 May 2024).
2. European Commission. An EU strategy on heating and cooling 2016. *J. Chem. Inf. Model.* **2016**, *53*, 1689–1699. [CrossRef]
3. European Parliament and Council. Directive 2010/31/EU of the European Parliament and of the Council of 19 may 2010 due on the energy performance of buildings. *Off. J. Eur. Union* **2010**, *153*, 13–35.
4. Schlomann, B.; Kleeberger, H. *Report: Energieverbrauch des Sektors Gewerbe, Handel, Dienstleistungen (GHD) in Deutschland für Die Jahre 2011 bis 2013*; Institute for Resource Efficiency and Energy Strategies: Karlsruhe, Germany, 2015; p. 30. Available online: https://irees.de/2020/06/15/energieverbrauch-des-sektors-gewerbe-handel-dienstleistungen-ghd-in-deutschland-fuer-die-jahre-2011-bis-2013-2015 (accessed on 1 May 2024).
5. Jouhara, H.; Yang, J. Energy efficient HVAC systems. *Energy Build.* **2018**, *179*, 83–85. [CrossRef]
6. Zhu, Y.; Wu, S.; Li, J.; Jia, Q.; Zhang, T.; Zhang, X.; Han, D.; Tan, Y. Towards a carbon-neutral community: Integrated renewable energy systems (IRES)–sources, storage, optimization, challenges, strategies and opportunities. *J. Energy Storage* **2024**, *83*, 110663. [CrossRef]
7. Olympios, A.V.; Song, J.; Ziolkowski, A.; Shanmugam, V.S.; Markides, C.N. Data-driven compressor performance maps and cost correlations for small-scale heat-pumping applications. *Energy* **2024**, *291*, 130171. [CrossRef]
8. Wen, Q.; Zhi, R.; Wu, Y.; Lei, B.; Ban, G. Experimental studies of semi hermetic single screw compressor with variable speed in heat pump. *Case Stud. Therm. Eng.* **2024**, *58*, 104399. [CrossRef]

9. Wu, C.; Li, X.; Wang, Z.; Xu, Z.; Xu, C.; Yang, Y. Optimizing the selection and combined operation of multiple air-source heat pumps for sustainable heating systems. *Energy Build.* **2024**, *310*, 114052. [CrossRef]
10. Koopman, T.; Zhu, T.; Rohlfs, W. Performance evaluation of air-source heat pump based on a pressure drop embed-ded model. *Heliyon* **2024**, *10*, e24634. [CrossRef]
11. Panteli, M.; Mancarella, P. Influence of extreme weather and climate change on the resilience of power systems: Impacts and possible mitigation strategies. *Electr. Power Syst. Res.* **2015**, *127*, 259–270. [CrossRef]
12. Pineda Quijano, D.; Fonseca Lima, B.; Infante Ferreira, C.; Brück, E. Seasonal COP of a residential magnetocaloric heat pump based on MnFePSi. *Int. J. Refrig.* 2024; *in press*. [CrossRef]
13. Wang, J.; Lu, X.; Adetola, V.; Louie, E. Modeling Variable Refrigerant Flow (VRF) systems in building applications: A comprehensive review. *Energy Build.* **2024**, *311*, 114128. [CrossRef]
14. Jain, N.; Alleyne, A.G. Thermodynamics-based optimization and control of vapor-compression cycle operation: Optimization criteria. In Proceedings of the 2011 American Control Conference, San Francisco, CA, USA, 29 June–1 July 2011; pp. 1352–1357. [CrossRef]
15. Jensen, J.B.; Skogestad, S. Optimal operation of simple refrigeration cycles. Part I: Degrees of freedom and optimality of sub-cooling. *Comput. Chem. Eng.* **2007**, *31*, 712–721. [CrossRef]
16. Aprea, C.; Mastrullo, R.; Renno, C. Experimental analysis of the scroll compressor performances varying its speed. *Appl. Therm. Eng.* **2006**, *26*, 983–992. [CrossRef]
17. Dongellini, M.; Abbenante, M.; Morini, G.L. A strategy for the optimal control logic of heat pump systems: Impact on the energy consumption of a residential building. In Proceedings of the 12th IEA Heat Pump Conference, Rotterdam, The Netherlands, 15–18 May 2017.
18. Xu, Z.; Li, H.; Xu, W.; Shao, S.; Wang, Z.; Gou, X.; Zhao, M.; Li, J. Investigation on the efficiency degradation characterization of low ambient temperature air source heat pump under partial load operation. *Int. J. Refrig.* **2022**, *133*, 99–110. [CrossRef]
19. Chae, S.; Bae, S.; Nam, Y. Performance improvement of air-source heat pump via optimum control based on artificial neural network. *Energy Rep.* **2023**, *10*, 460–472. [CrossRef]
20. Wang, W.; Hu, B.; Wang, R.Z.; Luo, M.; Zhang, G.; Xiang, B. Model predictive control for the performance improvement of air source heat pump heating system via variable water temperature difference. *Int. J. Refrig.* **2022**, *138*, 169–179. [CrossRef]
21. Hlanze, P.; Jiang, Z.; Cai, J.; Shen, B. Model-based predictive control of multi-stage air-source heat pumps integrated with phase change material-embedded ceilings. *Appl. Energy* **2023**, *336*, 120796. [CrossRef]
22. Putrayudha, S.A.; Kang, E.C.; Evgueniy, E.; Libing, Y.; Lee, E.J. A study of photovoltaic/thermal (PVT)-ground source heat pump hybrid system by using fuzzy logic control. *Appl. Therm. Eng.* **2015**, *89*, 578–586. [CrossRef]
23. Yang, T.; Ge, T. Performance study of a heat pump fresh air unit based on desiccant coated heat exchangers under different operation strategies. *Energy* **2024**, *296*, 131182. [CrossRef]
24. Rohrer, T.; Frison, L.; Kaupenjohann, L.; Scharf, K.; Hergenr, E. Deep Reinforcement Learning for Heat Pump Control. *arXiv* **2022**, arXiv:2212.12716. [CrossRef]
25. Park, C.; Lee, H.; Hwang, Y.; Radermacher, R. Recent advances in vapor compression cycle technologies. *Int. J. Refrig.* **2015**, *60*, 118–134. [CrossRef]
26. Al-Obaidi, A.S.M.; Naif, A.; Al-Harthi, T.K. Optimization of the Performance of Vapour Compression Cycle using Liquid Suction Line Heat Exchanger. *J. Therm. Eng.* **2020**, *6*, 201–210. [CrossRef]
27. Pottker, G.; Hrnjak, P. Experimental investigation of the effect of condenser subcooling in R134a and R1234yf air-conditioning systems with and without internal heat exchanger. *Int. J. Refrig.* **2015**, *50*, 104–113. [CrossRef]
28. Kwan, T.H.; Shen, Y.; Wu, Z.; Yao, Q. Performance analysis of the thermoelectric device as the internal heat exchanger of the trans-critical carbon dioxide cycle. *Energy Convers. Manag.* **2020**, *208*, 112585. [CrossRef]
29. Liu, X.; Fu, R.; Wang, Z.; Lin, L.; Sun, Z.; Li, X. Thermodynamic analysis of transcritical $CO_2$ refrigeration cycle integrated with thermoelectric subcooler and ejector. *Energy Convers. Manag.* **2019**, *188*, 354–365. [CrossRef]
30. Qureshi, B.A.; Zubair, S.M. The effect of refrigerant combinations on performance of a vapor compression refrigeration system with dedicated mechanical sub-cooling. *Int. J. Refrig.* **2012**, *35*, 47–57. [CrossRef]
31. Khan, J.U.R.; Zubair, S.M. Design and rating of an integrated mechanical-subcooling vapor-compression refrigeration system. *Energy Convers. Manag.* **2000**, *41*, 1201–1222. [CrossRef]
32. Huff, H.; Lindsay, D.; Radermacher, R. Positive displacement compressor and expander simulation. In Proceedings of the International Compressor Engineering Conference: 8 (Paper 1527), West Lafayette, IN, USA, 16–19 July 2002; Available online: https://docs.lib.purdue.edu/icec/1527/ (accessed on 26 February 2024).
33. Wang, M.; Zhao, Y.; Cao, F.; Bu, G.; Wang, Z. Simulation study on a novel vane-type expander with internal two-stage expansion process for R-410A refrigeration system. *Int. J. Refrig.* **2012**, *35*, 757–771. [CrossRef]
34. Boumaraf, L.; Haberschill, P.; Lallemand, A. Investigation of a novel ejector expansion refrigeration system using the working fluid R134a and its potential substitute R1234yf. *Energy Econ.* **2014**, *45*, 148–159. [CrossRef]
35. Cao, X.; Liang, X.; Shao, L.; Zhang, C. Performance analysis of an ejector-assisted two-stage evaporation single-stage vapor-compression cycle. *Appl. Therm. Eng.* **2022**, *205*, 118005. [CrossRef]
36. Cho, H.; Chung, J.T.; Kim, Y. Influence of liquid refrigerant injection on the performance of an inverter-driven scroll compressor. *Int. J. Refrig.* **2003**, *26*, 87–94. [CrossRef]

37. Pathak, A.; Binder, M.; Ongel, A.; Ng, H.W. Investigation of a multi stage vapour-injection cycle to improve air-conditioning system performance of electric buses. In Proceedings of the 14th International Conference on Ecological Vehicles and Renewable Energies, EVER, Monte-Carlo, Monaco, 8–10 May 2019; pp. 1–7. [CrossRef]
38. Lee, H.; Hwang, Y.; Radermacher, R.; Chun, H.H. Performance investigation of multi-stage saturation cycle with natural working fluids and low GWP working fluids. *Int. J. Refrig.* **2015**, *51*, 103–111. [CrossRef]
39. Yang, M.; Wang, B.; Li, X.; Shi, W.; Zhang, L. Evaluation of two-phase suction, liquid injection and two-phase injection for decreasing the discharge temperature of the R32 scroll compressor. *Int. J. Refrig.* **2015**, *59*, 269–280. [CrossRef]
40. Jacob, T.A.; Shah, N.; Park, W.Y. Evaluation of hybrid evaporative-vapor compression air conditioners for different global climates. *Energy Convers. Manag.* **2021**, *249*, 114841. [CrossRef]
41. Bagarella, G.; Lazzarin, R.; Noro, M. Sizing strategy of on-off and modulating heat pump systems based on annual energy analysis. *Int. J. Refrig.* **2016**, *65*, 183–193. [CrossRef]
42. Huang, B.; Jian, Q.; Luo, L.; Zhao, J. Experimental study of enhancing heating performance of the air-source heat pump by using a novel heat recovery device designed for reusing the energy of the compressor shell. *Energy Convers. Manag.* **2017**, *138*, 38–44. [CrossRef]
43. Wang, L.; Ma, G.; Ma, A.; Zhou, F.; Li, F. Experimental study on the characteristics of triplex loop heat pump for exhaust air heat recovery in winter. *Energy Convers. Manag.* **2018**, *176*, 384–392. [CrossRef]
44. Guoyuan, M.; Qinhu, C.; Yi, J. Experimental investigation of air-source heat pump for cold regions. *Int. J. Refrig.* **2003**, *26*, 12–18. [CrossRef]
45. Lee, Z.; Gupta, K.; Kircher, K.J.; Zhang, K.M. Mixed-integer model predictive control of variable-speed heat pumps. *Energy Build.* **2019**, *198*, 75–83. [CrossRef]
46. Clauß, J.; Georges, L. Model complexity of heat pump systems to investigate the building energy flexibility and guidelines for model implementation. *Appl. Energy* **2019**, *255*, 113847. [CrossRef]
47. Lee, S.H.; Jeon, Y.; Chung, H.J.; Cho, W.; Kim, Y. Simulation-based optimization of heating and cooling seasonal performances of an air-to-air heat pump considering operating and design parameters using genetic algorithm. *Appl. Therm. Eng.* **2018**, *144*, 362–370. [CrossRef]
48. Jensen, J.B.; Skogestad, S. Control and optimal operation of simple heat pump cycles. *Comput. Aided Chem. Eng.* **2005**, *20*, 1429–1434. [CrossRef]
49. Frik, A.; Bielskus, J.; Dzikevics, M. Experimental Study on the Control of the Positions of the Cycle Isotherms of the Heat Pump in the Air Handling Unit. *Environ. Clim. Technol.* **2023**, *27*, 889–899. [CrossRef]
50. Zhang, Y.; Li, M.; Dong, J.; Zhang, C.; Li, X.; Han, Z. Study on the impacts of refrigerant leakage on the performance and reliability of datacenter composite air conditioning system. *Energy* **2023**, *284*, 129336. [CrossRef]
51. Pelella, F.; Viscito, L.; Mauro, A.W. Combined effects of refrigerant leakages and fouling on air-source heat pump performances in cooling mode. *Appl. Therm. Eng.* **2021**, *204*, 117965. [CrossRef]


**Disclaimer/Publisher's Note:** The statements, opinions and data contained in all publications are solely those of the individual author(s) and contributor(s) and not of MDPI and/or the editor(s). MDPI and/or the editor(s) disclaim responsibility for any injury to people or property resulting from any ideas, methods, instructions or products referred to in the content.